Rheol Acta (2007) 46:1075–1082
DOI 10.1007/s00397-007-0196-5

ORIGINAL CONTRIBUTION

Rheological characterization of asphalt in a temperature-gradient combinatorial squeeze-flow setup

Yatin P. Patil · Antonio Senador · Patrick T. Mather · Montgomery T. Shaw

Received: 22 May 2006 / Accepted: 19 April 2007 / Published online: 12 May 2007

Abstract A new technique for parallel rheological characterization of asphalt in a combinatorial squeeze-flow array is described. The basis of the technique is a device that is capable of subjecting multiple samples simultaneously to constant volume (Type B) squeeze flow with application of a temperature gradient. The time-dependent sample dimensions, which are calculated from digital images taken through the transparent top plate, are used to derive the flow curves. The results obtained using the combinatorial setup compared favorably with those obtained using conventional parallel-plate torsional flow in a commercial rheometer. With the existing setup, the accessible shear rate range is limited to about one decade at a single temperature.

Keywords Combination rheometer · Squeeze flow · Asphalt

Introduction

Asphalt is the heavy "bottoms" product from petrochemical refineries and is used predominantly as a binder for roads. Its properties depend on the composition of the feed stock and the processing parameters. Not surprisingly, it is a complex material containing aliphatic and aromatic saturated and unsaturated polar and nonpolar organic compounds. The supermolecular structure is thought to be a three-dimensional network of asphaltenes dispersed in maltenes (Shen 1996). Asphaltenes comprise the hexane- or heptane-insoluble fraction and are aggregates of polar aromatic compounds (Maruska and Rao 1987). Maltenes are nonpolar aliphatic hydrocarbons soluble in hexane or heptane.

Asphalt is graded for a particular temperature range as a road binder using standardized mechanical tests (American Association of State Highway Officials 2002). Although simple in concept, these tests involve expensive equipment and are exceedingly time consuming. The tests are protracted mainly because asphalt undergoes considerable structural changes due to physical aging (VanderHart et al. 1990; Lin et al. 1996). Work done by other groups has shown that asphalt requires isothermal annealing for extended periods (>10 h) before rheological measurements, thus consuming valuable instrument time (Anderson and Marasteanu 1999). Because of their codification, the conventional tests will continue to be used. However, considerable time could be saved by a quick prescreening process to eliminate batches of asphalt that are unlikely to meet the required specifications. A simpler quicker test would therefore be beneficial.

No matter how simple the test, conventional rheometers lack the ability to characterize multiple samples simultaneously, and most require that the sample be annealed in the fixtures. To alleviate this problem, there is a need for simultaneous analysis of materials under an array of test variables. With such a procedure, one can test samples in a combinatorial fashion under a stress and temperature gradient in minutes per sample as opposed to hours

This paper was presented at the Third Annual European Rheology Conference, April 27–29, 2006, Crete, Greece.

Y. P. Patil · M. T. Shaw
Polymer Program, Institute of Materials Science,
University of Connecticut,
Storrs, CT, USA

A. Senador · M. T. Shaw (✉)
Chemical Engineering Program, Department of Chemical Materials and Biomolecular Engineering,
University of Connecticut,
Storrs, CT, USA
e-mail: montgomery.shaw@uconn.edu

P. T. Mather
Macromolecular Science, Case Western Reserve University,
Cleveland, OH, USA

required by conventional rheometers. Different materials can be analyzed and compared in a single experimental run, which can reduce error connected with resolving small differences between the samples. In addition, reference materials can be seeded among the cells in the array.

The combinatorial approach is broadly applied in synthesis, but for characterization, it is not as popular. Only a few studies have been reported for parallel rheological characterization (Breedveld and Pine 2003; Pathak et al. 2005; Walls et al. 2005), and there is but a small amount of patent activity (e.g., Hajduk et al. 2002; Kolosov and Matsiev 2004) on devices for the characterization of solids or melts. Application of these to asphalt characterization has not, to our knowledge, been attempted.

One of the less conventional methods used for characterizing materials is squeeze flow (Scott 1931; Peek 1932; Dienes and Klemm 1946; Gent 1960; Leider and Bird 1974; Shaw 1977; Kataoka et al. 1978; Winther et al. 1991; Laun 1992; Laun et al. 1999; Meeten 2002; Sherwood 2005). While its nonuniform and unsteady flow field has discouraged commercialization, it does have several distinct advantages for testing asphalt. For example, the sample is placed between two disposable plates meaning that all sample preparation loading and annealing can be done externally to the rheometer, and the tested sample can be discarded along with the plates without the need for cleaning the equipment.

Most squeeze-flow geometries involve radial flow of disc-shaped samples between two parallel plates under a constant normal force or constant approach velocity. By measuring the applied load, sample volume, and the change in the thickness as a function of time, the shear stress and shear rate can be approximated. Two types of squeeze flow, namely, constant diameter and constant volume (Fig. 1), have been analyzed (e.g., Scott 1931; Dienes and Klemm 1946; Gent 1960; Leider and Bird 1974; Winther et al. 1991; Laun et al. 1992; Sherwood 2005). In the former, the diameters of the sample and plates are same; the material squeezed out of the plates is ignored. The vast majority of the squeeze-flow studies reported are based on constant-volume (Type A) squeeze flow. In constant-volume squeeze flow, the sample diameter is smaller than the plate diameter and material never flows out of the plates; thus, the volume of sample subjected to squeezing remains same. In this type, one can track either the decrease in gap or increase in sample radius, whereas the constant-diameter method requires direct measurement of the gap. For the squeezing of a power-law fluid in this geometry, an analytical solution known as the Scott equation applies in the lubrication approximation limit (Scott 1931).

The specific objective of this work was to develop a fast and simple combinatorial setup for parallel characterization of asphalt under an array of test variables. Using constant-volume squeeze flow, multiple samples in a temperature gradient arrangement were simultaneously subjected to squeeze flow to assess their rheological behavior. The results obtained using the combinatorial setup were then compared with those obtained using dynamic torsional flow between parallel plates in a conventional rheometer.

Experimental

Instrumental setup

Figure 2 shows the combinatorial setup used for this study. The foundation of the apparatus is Plate A, which was fabricated of heavy aluminum to minimize temperature gradients across individual specimens. Slots were cut in the plate perpendicular to the temperature gradient to minimize heat flow between the rows. The vacuum port in Plate A connects to a vacuum pump. A large flask was incorporated in the vacuum line to help increase the rate of application of the partial vacuum to the space between the bottom (Plate A) and the membrane. A vacuum regulator was installed to control the pressure and, thus, the force on the membrane, while a mercury manometer was used to monitor this pressure. For all experiments described in this report, the

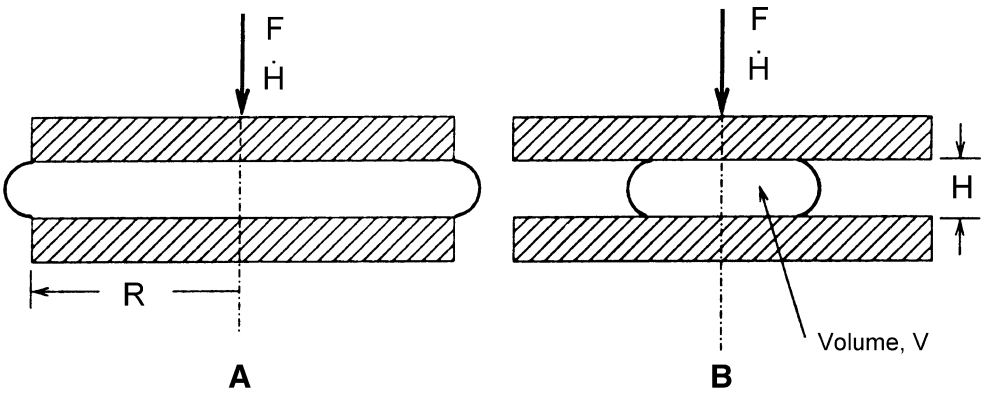

Fig. 1 Two types of squeeze flow constant radius (Type A) and constant volume (Type B). During squeezing, the radius R in the Type B geometry increases while that in A remains constant

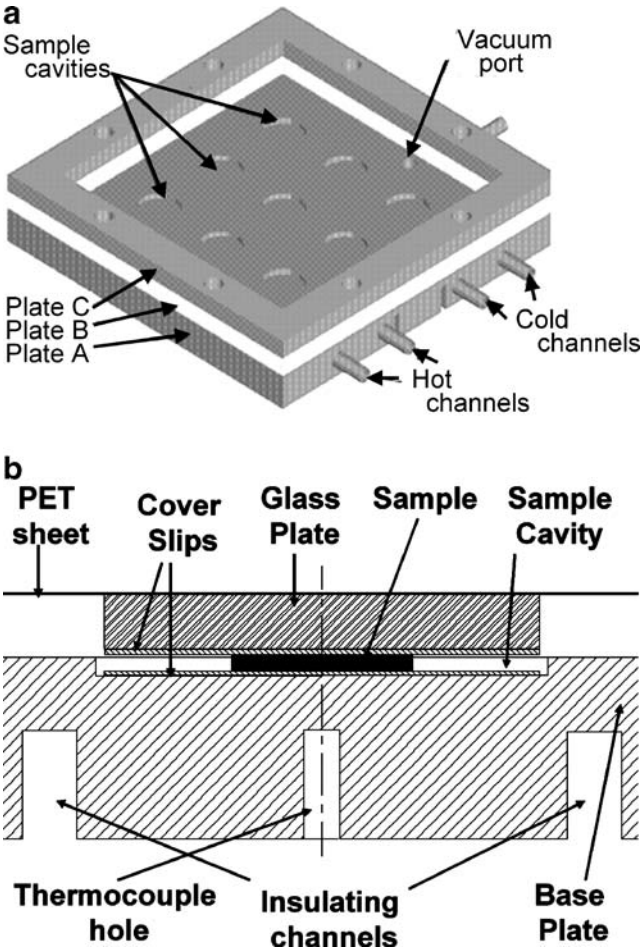

Fig. 2 Combinatorial instrumental setup. **a** Pictorial view and **b** cross-section of one cell

absolute pressure was held at 76 mm. Plate B functioned as a spacer to hold a thin transparent polyethylene terephthalate film such that it just touched the sample cells, one of which is illustrated in Fig. 2b. Plate C functioned as a clamp to hold the membrane tightly against Plate B. Rubber gaskets were placed between Plate A and Plate B and between the membrane and Plate B to prevent leakage. Eight Allen screws clamped the assembly together.

Nine circular cavities 1 mm deep were machined in Plate A to position the samples in three rows of three cells each. To test samples simultaneously at different temperatures, it was necessary to establish a temperature gradient across the array of cells. The temperature gradient was achieved by circulating hot water underneath the left-hand row of cells positioned in Plate A and cold water under the right-hand row, as shown in Fig. 2a. Thermocouples were embedded in Plate A below each sample cavity to check on the actual temperature. To calibrate the thermocouples, dummy asphalt samples each containing very thin thermocouples were sandwiched between two circular coverslips and placed in the sample cavities. After applying the chosen partial vacuum and achieving the desired plate temperature gradient, both the sample temperatures and plate temperatures below each sample cavity were measured. This procedure provided a correction for the sample temperature relative to the plate temperature. The entire setup was placed in insulating foam to control heat losses from the edges.

Sample diameters were recorded at desired intervals using a Nikon D70 digital SLR camera. The camera was connected to a computer via a universal serial bus (USB) and was controlled by Nikon Capture 4 camera control software. Every image file had embedded time information, which was used for shear rate calculation.

Force computation

The force experienced by each sample under the applied partial vacuum was established based on the deflection of calibrated wave washers that were substituted for the samples (Fig. 3a). A load vs deflection calibration curve was recorded beforehand for each washer using an Instron tensile tester. At each sample station, the washer and a pre-weighed sample of silicone polymer (SE 30) were placed between two glass coverslips. A 25-mm-diameter 4-mm-thick glass plate was placed on top of the coverslips. The purpose of the silicone sample was to register the thickness change brought about by the compression of the wave washer due to the application of the partial vacuum. As with the asphalt samples, the area before and after application of the partial vacuum was measured by taking pictures using a digital camera (Fig. 3a). During these experiments, the other sample cavities had coverslips and glass plates to position the membrane correctly. Figure 3b shows the average value of the force experienced by the nine samples and their positions in the setup. The force experienced by the center sample is highest as the cover film has minimum edge constraints at this position. Clearly in a larger array, the forces at each station would be virtually constant.

Sample preparation

Standardized asphalt samples (PG 76-28) were obtained from the Connecticut Advanced Pavement Laboratory (http://www.engr.uconn.edu/ti/ti/CAPLab/caplab_staff.html). As asphalt is very difficult to handle, we adopted a form-and-freeze technique to prepare the required disk-shaped test units. In 0.5-, 1-, and 1.5-mm-thick aluminum plates, 6-, 9-, 12-, and 15-mm holes were drilled to serve as molds to make the asphalt disks. The plates were coated with a mold release agent Chemlease-PMR from Chem-Trend Release Innovations. The plate, along with the asphalt, was placed between two Teflon sheets and kept in a hot press for 10 min at 60 °C. After removing the assembly

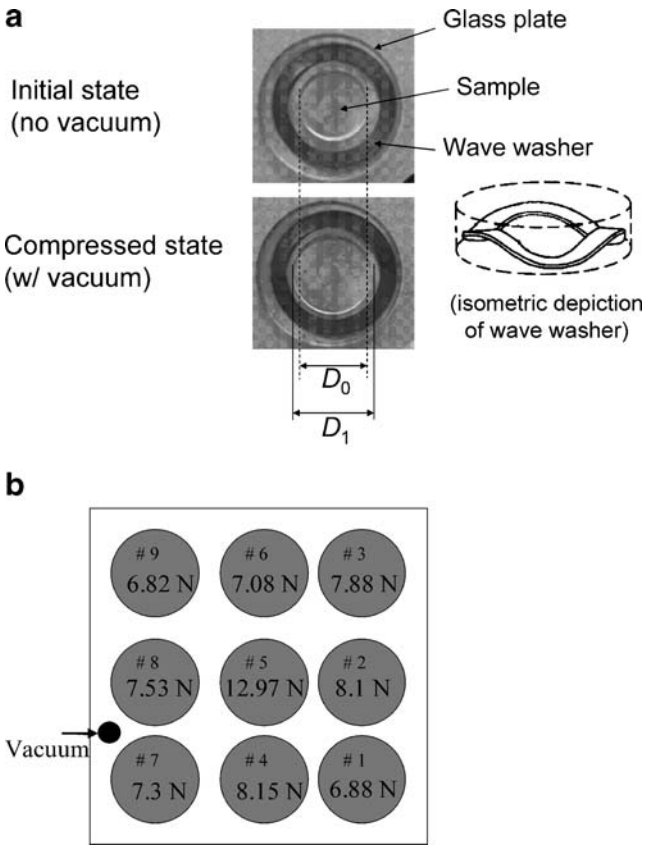

Fig. 3 **a** Images of a squeeze cell before and after application of partial vacuum. The clear sample of silicone has been squeezed in the bottom photo to a larger diameter D_1 than the starting size D_0 in the top photo. The *dark ring* is the wave washer, which is compressed in the bottom photo by a ratio $(D_1/D_0)^2$. The *inset* is a sketch of a wave washer. **b** Sample positions and the average force calculated from the deflection of wave washers

from hot press, it was cooled in dry ice for 5 min. The asphalt disks were ejected under cold conditions and placed between two pre-weighed coverslips. These sandwiches were annealed at 60 °C for 5 min to erase their thermal history. After cooling, the specimens were weighed and placed in the combinatorial setup. The sample volume was calculated from its weight and density.

Density at elevated temperature

Asphalt density in the range of 30 to 70 °C was measured using a dilatometer accessory in a Perkin Elmer Thermo Mechanical Analyzer TMA-7. The dilatometer dimensions were measured, and it was filed with asphalt sample PG 76-28. The sample was heated, cooled, and reheated from 30 to 70 °C at rate of 1 °C/min. The density values obtained from the second heating run were used for thickness calculations. Assuming a constant expansion coefficient gave the result:

$$\rho = \rho_0 \exp\left[-\alpha(T - T_0)\right] \tag{1}$$

with ρ_0=1.0344 g/cm^3 and α=0.00107 K^{-1} when T_0 is 30 °C.

Test procedure

The temperatures of the water baths were adjusted to achieve the desired temperature gradients. The discs were placed in the sample cavities for 20 min to equilibrate with the plate temperature. After clamping the three plates, the image acquisition was started followed by application of the partial vacuum. The experiment was continued for 20 min. The images, recorded in Joint Photographic Experts Group (JPEG) format, were analyzed using Image J 1.34S image analysis software available from the National Institutes of Health website. A metal disc of known diameter was placed in the setup as a calibration standard. The sample thickness was computed from the sample area, weight, and density. The sample diameters and thicknesses in an array were selected to cover as wide a shear rate range as practical. This proved to be about 1 to 1 1/2 decades (see Fig. 8).

Results and discussion

Figure 4 shows the images recorded during a squeeze-flow run. The samples on the right side of the images were on the heated side of the plate, while those on the left side were cooled. In this run, the temperatures for the three rows of samples were 20, 40, and 61 °C. Some time after the application of partial vacuum, a few of the samples flowed out of the disc, and the data beyond that point were not considered in the analysis. The samples along the low-temperature side never reached the edge of the disc. The increase in the sample area obtained from image analysis is shown in Fig. 5. The data sets that appear truncated are those where the sample reached the edge of the discs. Using area, density, and weight of individual samples, the thickness was calculated as a function of time (Fig. 6). As expected, the initial thicknesses of the cold samples were close to the thickness of the mold used to form them. However, samples at elevated temperatures exhibited some flow during the setup due to their low viscosities.

Based on constant volume squeeze flow equations, the rim shear rate and rim shear stress were calculated as follows (Kataoka et al. 1978; Laun 1992):

$$\sigma_R = \left[\frac{n+3}{4}\right]\left[\frac{H^{5/2}F}{\pi(V/\pi)^{3/2}}\right] \tag{2}$$

$$\dot{\gamma}R = \left[\frac{2(2n+1)}{3n2^{1/n}}\right]\left[\frac{3(-\mathrm{d}H/\mathrm{d}t)(V/\pi)^{1/2}}{2H^{5/2}}\right] \tag{3}$$

In these equations, n is the power-law exponent (Eq. 7), H is the sample thickness at time t, F is the applied force,

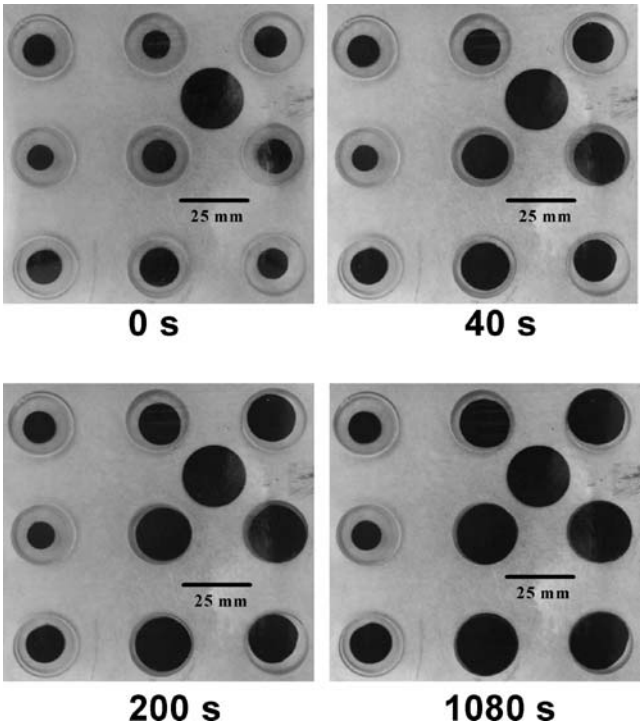

Fig. 4 Images taken during a combinatorial squeeze flow run at the times indicated. The partial vacuum is 76 mmHg, while the temperatures of the vertical rows are 20, 40, and 61 °C left to right. The *black circle* in the upper right quadrant is a size scale reference

and V is the volume of the sample. The value of n may be calculated from the slope of a plot of log ($-\mathrm{d}H/\mathrm{d}t$) vs log H. For a power-law fluid, such a plot yields a straight line (Scott equation) with a slope s of $5(n+1)/2n$, from which the power-law index is calculated as $n=5/(2s-5)$. A disadvantage of this approach is that the gap data must be differentiated twice—once to get $\mathrm{d}H/\mathrm{d}t$ and again to get the final value of n—which is likely to increase error. An advantage is that it can reveal changes in the power-law constants with time (or stress).

Alternatively, one can assume that the power-law parameters are invariant and integrate the Scott equation for Type B squeeze flow

$$F=\frac{\left(-\dot{H}\right)^{n}}{H^{\frac{5(n+1)}{2}}}\left(\frac{2n+1}{2n}\right)^{n}\frac{2^{n+1}\pi}{n+3}\left(\frac{V}{\pi}\right)^{\frac{n+3}{2}}m \tag{4}$$

to yield:

$$H(t;m,n)=\frac{H_0}{\left[1+H_0^{a}Kat\right]^{1/a}} \tag{5}$$

where H_0 is the initial gap, $a=(3n+5)/2n$, and the constant K is given by the equation

$$K=\frac{n}{2n+1}\left[\frac{(n+3)F}{2\pi m(V/\pi)^{\frac{n+3}{2}}}\right]^{1/n} \tag{6}$$

The symbols m and n represent the parameters in the usual power-law expression

$$\eta=m\dot{\gamma}^{n-1} \tag{7}$$

where η is the viscosity, and $\dot{\gamma}$ is the magnitude of the shear rate. One can then find m and n by nonlinear regression of the gap vs time data using Eqs. 5 and 6. The initial gap H_0 can also be treated as a parameter as it may not be known very accurately. Note that any time can be used as zero time and the corresponding estimated gap at that time will be H_0.

Pursuing the differential method, we calculated numerically the values of $\mathrm{d}H/\mathrm{d}t$ using a moving five-point quadratic applied to both $H(t)$ vs t and log $H(t)$ vs t data sets. The slopes derived from these two were substantially the same, which verified the differentiation method. The double log plots corresponding to Fig. 6 are shown in the Fig. 7.

The integral method proved to be surprisingly effective (see Fig. 6b). Convergence was obtained easily even with the initial gap as an unknown parameter. The results for the two methods are listed in Table 1 and show reasonable agreement. For both the dynamic and squeeze flow data, the power-law exponent n tended to increase with temperature ($P=0.008$[1]), i.e., the material became more Newtonian. The dynamic and squeeze flow results at 40 and 60 °C were indistinguishable. Running the asphalt on the rheometer at 20 °C proved to be difficult, but the dynamic results at 30 °C suggest that the squeeze flow test tends to give viscosities that are too low and with excessive shear thinning, relative to the dynamic results. Slip is a possible cause (Laun et al. 1999); tilt in the plates is another (Hoffner et al. 2001). The former might be due to residual mold release, which would reduce the shear stress gradient responsible for the radial pressure drop. Tilt, on the other hand, opens up an easy flow path on the high side as a result of the highly nonlinear gap dependence (see Eq. 4).

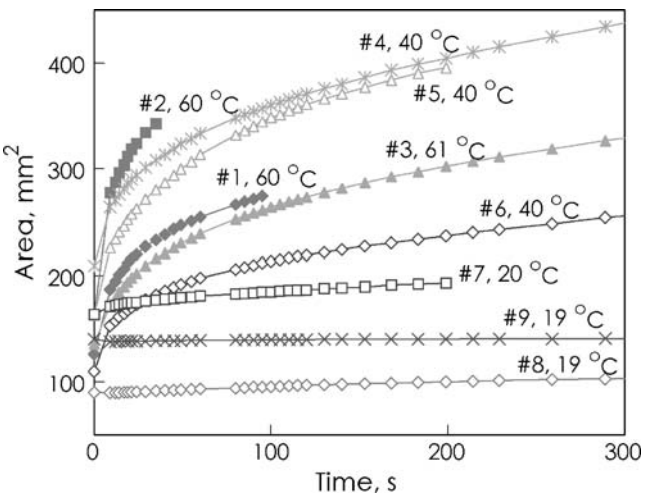

Fig. 5 Sample area change as a function of time during a squeeze-flow run

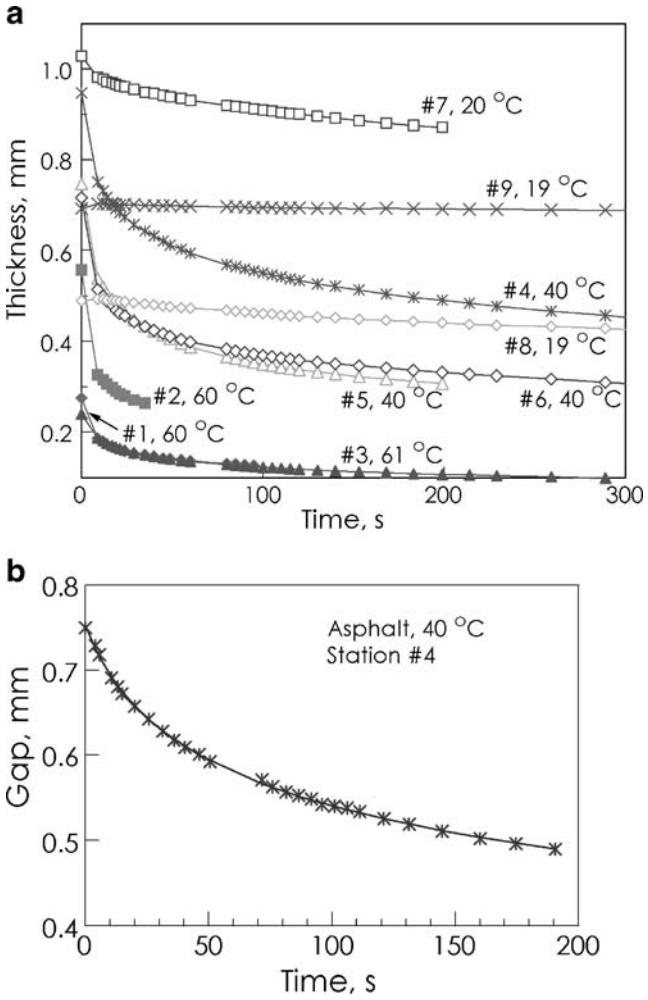

Fig. 6 **a** Sample thickness during a single combinatorial squeeze-flow run derived from area; and **b** example fit of the integral form of the Scott equation to observations for Station #4. The first point has been eliminated, and the time scale shifted. Power-law constants: m=7070±400 and n=0.572±0.024. Initial gap: 0.735±0.008 mm

Figure 8 displays a comparison between the results obtained using a combinatorial setup and those obtained using a parallel-plate rheometer under dynamic mode. The curves containing symbols connected by lines are the viscosities obtained from squeeze flow setup, while the curves represented by the relatively straight dashed lines without any symbols are values for the magnitude of complex viscosities. The samples at 40 and 60 °C covered a shear rate range of one decade, whereas samples at 20 °C covered a shear rate range of more than two decades. At elevated temperatures, the samples did not retain their initial shape and also squeezed out of the discs due to low viscosity. This reduced the number of available data point for the calculations which, in turn, reduced the available shear rate range. The limitations can be overcome by using a smaller sample such that the asphalt does not squeeze out. The irregular nature of some of the flow curves obtained for different samples using the combinatorial apparatus is due to the fact that these curves are constructed point by point from raw sample thickness data and values of the differential at each thickness.

Figure 9 compares calculated viscosity values at a stress of 10 kPa for the two methods assuming the validity of the Cox–Merz relationship, that is, $|\eta^*|\omega$=10 kPa for the dynamic method, where $|\eta^*|$ is the magnitude of the complex viscosity, and ω is the angular frequency. While the agreement is satisfactory, there is a suggestion that the squeeze-flow experiment may lead to somewhat lower viscosity values.

The results obtained from the dynamic tests show that asphalt exhibits nearly perfect power-law behavior. Hence, a power-law approximation for the squeeze-flow analysis is a reasonable one, although the asphalt sample used does exhibit a slight degree of elasticity (G'>0). For highly elastic materials, the results may be less satisfactory, although squeezing flow has been applied to viscoelastic polymer melts (e.g., Leider and Bird 1974; Winther et al. 1991; Laun 1992). In most cases, squeezing flow has been quite successful for characterizing the steady shearing response of these melts at low to moderate shear rates and, thus, complements the capillary rheometer.

While there were no discernable trends with sample size or force values, there was evidence of tilting of the plates at some stations particularly Station #5, as evidenced by thickness measurements on completion of the run. The different power-law exponent for this sample compared to the other two samples at similar temperature could have resulted from this problem. Tilt may develop during the

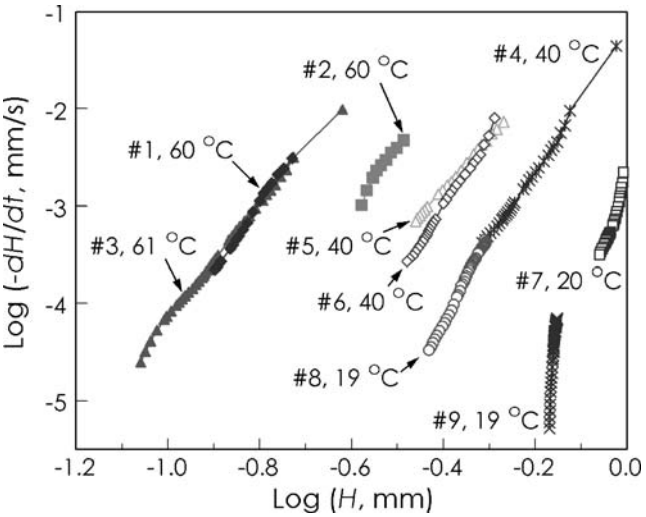

Fig. 7 Double log plot of (−dH/dt) vs H for the nine samples

[1] Probability of a Type I error, that is, the fractional chance of being in error by rejecting the hypothesis that there is no change in n with temperature.

Table 1 Summary of power-law constants and viscosities derived from squeeze flow and from dynamic data

Station #	Samplewt. (g)	Temperature (°C)	Differential method		Integral method		Dynamic data	
			m (Pa s^n)	n	m (Pa s^n)	n	m (Pa s^n)	n
1	0.0349	60	890	0.50	878	0.53		
2	0.9098	60	–[a]	–[a]	1,270	0.55		
3	0.0325	61	1,280	0.75	1,270	0.75		
Average		60			1,140	0.61	1,130	0.65
Visc. @ 10 kPa		60			0.28		0.35[b]	
4	0.2026	40	7,180	0.56	7,070	0.57		
5	0.1244	40	8,010	0.75	8,720	0.80		
6	0.0805	40	10,100	0.65	10,000	0.65		
Average		40			8,600	0.67	10,900	0.59
Visc. @ 10 kPa		40			8.0		11.6[b]	
7	0.1753	20	15,700	0.21	16,700	0.22		
8	0.0461	19	42,000	0.38	35,900	0.35		
9	0.1013	19	8,600	0.028	15,400	0.12		
Average		19			23,000	0.23	39,500[c]	0.565[c]
Visc. @ 10 kPa		19			374		114[b,c]	

Power law constant n is dimensionless. The units of m change with the value of n and are Pa s^n in this table. Thus, for the first entry, m=890 Pa s$^{0.5}$.
[a] Insufficient data
[b] Value of $|\eta^*|$ @ $|\eta^*|\omega$=10 kPa.
[c] Actual temperature=30 °C

annealing step, or the sample may simply be off center. For samples that do not reach the edge, the degree of tilt can be determined after the run, and corrections for slightly tilted plates have been published (Hoffner et al. 2001). The tilt could also be a result of an undesirable temperature gradient across the diameter of the sample, but the thick aluminum plate under each sample should have minimized this problem.

For the highly viscous samples such as asphalt at low temperatures, more motion of the plates can be achieved by lubrication, perhaps with fluorocarbon oil. The deformation then approaches uniform biaxial and can be analyzed with viscoelastic constitutive models.

As a final note, it is readily shown that the shear rate and stress shown in Eqs. 2 and 3 are not what one would surmise for flow through a channel with a "width" of $2\pi R$

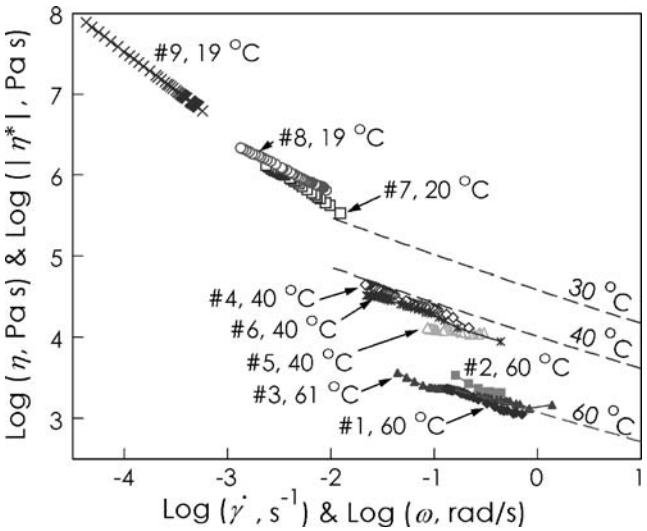

Fig. 8 Comparison of viscosity results obtained from combinatorial rheometer with the magnitude of the complex viscosity (*dotted lines*) obtained using parallel-plate fixtures in an Advanced Rheometric Expansion System (ARES) rheometer

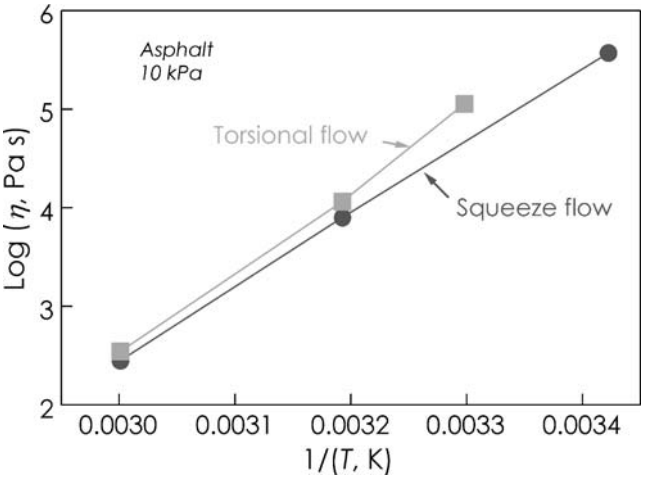

Fig. 9 Viscosity changes with temperature for asphalt as measured by the two techniques at a stress of 10 kPa. The Cox–Merz relationship is assumed for conversion of the complex viscosity magnitude to steady shear viscosity

and a flow rate of $\pi R^2\left(-\dot{H}\right) = V\left(-\dot{H}\right)\Big/H$. The two differ by a factor of $2^{1/n}$ and 2, respectively, yielding a viscosity that differs by a ratio of $2/2^{1/n}$. The effect of this difference is to move the viscosity to higher values at lower shear rates while leaving the power-law constants m and n untouched. Laun et al. (1992) credit the source of Eqs 2 and 3 to a paper by Kataoka et al. (1978), and this was verified. However, the latter authors do not derive or explain the equations in this paper but refer the reader to two other sources. Inspection, in turn, of these sources did not result in any clarification of the issue, as both appeared to address plastic materials only.

Conclusions

Based on the Type B squeeze flow technique with vacuum actuation, we have demonstrated a simple combinatorial method for parallel rheological characterization of high-viscosity fluids. The results obtained using the technique for asphalt samples at different temperature were consistent with the conventional single-sample rheometer. The existing combinatorial setup could only cover a shear rate range of about one decade at elevated temperatures. However, one could easily fabricate arrays that would accommodate discs of different size to cover a wider shear rate range. Clearly, also the partial vacuum level used for actuation could be increased or decreased to achieve different stress levels, but estimates indicate that with a given disc size only about two decades of shear stress can be covered using the feasible range of partial vacuum and sample size.

As the array size increases, more variables including different asphalts and reference samples could be included along with temperature and stress variations. While the asphalt samples provided optimal optical contrast, it was also shown that transparent materials can also be characterized. Problems with nonparallelism were experienced, but symmetry suggests that these may be minimized, as the array is expanded. Also recorded is the integral form resulting from integration of the Type B power-law equation based on the lubrication approximation.

Acknowledgements We gratefully acknowledge the financial support of the Joint Research Advisory Council of the University of Connecticut and the Connecticut Department of Transportation. We also thank Jim Mahoney at the Connecticut Advanced Pavement Laboratory for providing the standardized asphalt samples.

References

American Association of State Highway Officials (2002) Standard specification for performance graded asphalt binder MP1a-02 1–4

Anderson DA, Marasteanu MO (1999) Physical hardening of asphalt binders relative to their glass transition temperatures. Transp Res Rec 1661:27–34

Breedveld V, Pine DJ (2003) Microrheology as a tool for high-throughput screening. J Mater Sci 38:4461–4470

Dienes GJ, Klemm HF (1946) Theory and application of the parallel plate plastometer. J Appl Phys 4:257–264

Gent AN (1960) Theory of the parallel plate viscometer. Br J Appl Phys 11:85–87

Hajduk D, Carlson E, Srinvasan R (2002) Rheometer for rapidly measuring small quantity samples. US Patent 6,484,567

Hoffner BC, Campanella OH, Corradini MG, Peleg M (2001) Squeezing flow of a highly viscous fluid between two slightly inclined lubricated wide plates. Rheol Acta 40:289–295

Kataoka T, Kitano T, Nishimura T (1978) Utility of parallel-plate plastometer for rheological study of filled polymer melts. Rheol Acta 17:626–631

Kolosov O, Matsiev L (2004) High throughput rheological testing of materials. US Patent Application 2004123650

Laun HM (1992) Rheometry towards complex flows: squeeze flow technique. Makromol Chem Macromol Symp 56:55–66

Laun HM, Rady M, Hassager O (1999) Analytical solutions for squeeze flow with partial wall slip. J Non Newton Fluid Mech 81:1–15

Leider PJ, Bird RB (1974) Squeezing flow between parallel disks. I. Theoretical analysis. Ind Eng Chem Fundam 13:336–341

Lin M-S, Chaffin JM, Liu M, Glover CJ, Davison RR, Bullin JA (1996) The effect of asphalt composition on the formation of asphaltenes and their contribution to asphalt viscosity. Fuel Sci Technol Int 14:139–162

Maruska HP, Rao BML (1987) The role of polar species in the aggregation of asphaltenes. Fuel Sci Technol Int 5:119–168

Meeten GH (2002) Constant-force squeeze flow of soft solids. Rheol Acta 41:557–566

Pathak JA, Berg RF, Beers KL (2005) Development of a microfluidic rheometer for complex fluids. Am Chem Soc Polym Mater Sci Eng (PMSE) Preprints 93:972

Peek RL (1932) Parallel plate plastometry. J Rheol 3:345–372

Scott JR (1931) Theory and application of the parallel-plate plastometer. Trans Inst Rubber Ind 7:169–186

Shaw MT (1977) Melt characterization of ultra high molecular weight polyethylene using squeeze flow. Polym Eng Sci 17:266–268

Shen EY (1996) Physics of asphaltene micelles and microemulsions—theory and experiment. J Phys Condens Matter 8:A125–A141

Sherwood JD (2005) Model-free inversion of squeeze-flow rheometer data. J Non Newton Fluid Mech 129:61–65

VanderHart DL, Manders WF, Campbell GC (1990) Investigation of structural inhomogeneity and physical aging in asphalts by solid-state NMR. Am Chem Soc Div Petrol Chem Preprints 35(3):445–452

Walls HJ, Berg RF, Amis EJ (2005) Multi-sample Couette viscometer for polymer formulations. Meas Sci Technol 16:137–143

Winther G, Almdal K, Kramer O (1991) Determination of polymer melt viscosity by squeezing flow with constant plate velocity. J Non Newton Fluid Mech 39:119–136